BIOCHEMICAL PHARMACOLOGY 73 (2007) 1796–1806

available at www.sciencedirect.com

journal homepage: www.elsevier.com/locate/biochempharm

Inhibition of lipopolysaccharide-stimulated NO production by a novel synthetic compound CYL-4d in RAW 264.7 macrophages involving the blockade of MEK4/JNK/AP-1 pathway

Meng-Wei Lin [a], *Lo-Ti Tsao* [b], *Ling-Chu Chang* [c], *Ye-Long Chen* [d], *Li-Jiau Huang* [a], *Sheng-Chu Kuo* [a], *Cherng-Chyi Tzeng* [d], *Miau-Rong Lee* [e], *Jih-Pyang Wang* [a,b,*]

[a] *Graduate Institute of Pharmaceutical Chemistry, China Medical University, Taichung, Taiwan, ROC*
[b] *Department of Education and Research, Taichung Veterans General Hospital, Taichung, Taiwan, ROC*
[c] *Institute of Medicine, Chung Shan Medical University, Taichung, Taiwan, ROC*
[d] *Faculty of Medicinal and Applied Chemistry, Kaohsiung Medical University, Kaohsiung, Taiwan, ROC*
[e] *Department of Biochemistry, China Medical University, Taichung, Taiwan, ROC*

ARTICLE INFO

Article history:
Received 17 January 2007
Accepted 15 February 2007

Keywords:
CYL-4d
RAW 264.7 macrophages
Nitric oxide
AP-1
NF-κB
BV-2 microglia
Alveolar macrophages

ABSTRACT

In the present study, a novel synthetic compound 4-(2-(cyclohex-2-enylidene)hydrazinyl)-quinolin-2(1*H*)-one (CYL-4d) was found to inhibit lipopolysaccharide (LPS)-induced nitric oxide (NO) production without affecting cell viability or enzyme activity of expressed inducible NO synthase (iNOS) in RAW 264.7 macrophages. CYL-4d exhibited parallel inhibition of LPS-induced expression of iNOS protein, iNOS mRNA and iNOS promoter activity in the same concentration range. LPS-induced activator protein-1 (AP-1) DNA binding, AP-1-dependent reporter gene activity and c-Jun nuclear translocation were all markedly inhibited by CYL-4d with similar efficacy, whereas CYL-4d produced a weak inhibition of nuclear factor-κB (NF-κB) DNA binding, NF-κB-dependent reporter gene activity and p65 nuclear translocation without affecting inhibitory factor-κBα (IκBα) degradation. CYL-4d had no effect on the LPS-induced phosphorylation of extracellular signal-regulated kinase (ERK), p38 mitogen-activated protein kinase (MAPK) and its upstream activator MAPK kinase (MEK) 3, whereas it significantly attenuated the phosphorylation of c-Jun, c-Jun NH_2-terminal kinase (JNK) and its upstream activator MEK4 in a parallel concentration-dependent manner. Other Toll-like receptors (TLRs) ligands (peptidoglycans, double-stranded RNA, and oligonucleotide containing unmethylated CpG motifs)-induced iNOS protein expression were also inhibited by CYL-4d. Furthermore, the NO production from BV-2 microglial cells as well as rat alveolar macrophages in response to LPS was diminished by CYL-4d. These results indicate that the blockade of

* *Corresponding author at*: Department of Education and Research, Taichung Veterans General Hospital, Taichung, Taiwan, ROC. Tel.: +886 4 23592525x4023; fax: +886 4 23592705.
E-mail address: w1994@vghtc.gov.tw (J.-P. Wang).

Abbreviations: AP-1, activator protein-1; COX, cyclooxygenase; CYL-4d, 4-(2-(cyclohex-2-enylidene)hydrazinyl)quinolin-2(1*H*)-one; ERK, extracellular signal-regulated kinase; LPS, lipopolysaccharide; IκBα, inhibitory factor-κBα; IKK, IκB kinase; iNOS, inducible NO synthase; JNK, c-Jun NH_2-terminal kinase; MAPK, mitogen-activated protein kinase; MEK, MAPK kinase; NF-κB, nuclear factor-κB; NO, nitric oxide; Q-RT-PCR, quantitative real-time reverse transcription-polymerase chain reaction; TLR, Toll-like receptor

0006-2952/$ – see front matter
doi:10.1016/j.bcp.2007.02.009

NO production by CYL-4d in LPS-stimulated RAW 264.7 cells is attributed mainly to interference in the MEK4-JNK-AP-1 signaling pathway. CYL-4d inhibition of NO production is not restricted to TLR4 activation and immortalized macrophage-like cells.

1. Introduction

Inflammation is a central feature of many pathophysiological conditions in response to tissue injury and host defenses against invading microbes. Macrophages are the main pro-inflammatory cells responsible for invading pathogens by releasing many pro-inflammatory molecules, including the short-lived free radical nitric oxide (NO). NO is a product of the oxidation of L-arginine to L-citrulline catalyzed by nitric oxide synthase (NOS). Three isoforms of NOS have been identified: two constitutive NOS, endothelial NOS (eNOS) and neuronal NOS (nNOS), which are regulated by Ca^{2+}, and one inducible NOS (iNOS), which is independent of Ca^{2+} regulation [1]. Activated macrophages transcriptionally express iNOS, which is responsible for the prolonged and profound production of NO [2]. The aberrant release of NO can lead to amplification of inflammation, as well as tissue injury [3]. Therefore, pharmacological interference in expression of iNOS presents a promising chemotherapeutic strategy to control the potentially harmful pro-inflammatory activity of macrophages.

Despite the fact that there have been many efforts to develop anti-inflammatory agents, there are still a large demand for developing new agents. In the study of the anti-inflammatory activities of chemical synthetic quinolin-2(1*H*)-one (carbostyril) derivatives [4], some have been shown to inhibit the growth of several human cancer cell lines, we found that an intermediate product 4-(2-(cyclohex-2-enylidene)hydrazinyl)quinolin-2(1*H*)-one (CYL-4d) (Fig. 1), inhibited the Gram-negative bacterial cell wall component lipopolysaccharide (LPS)-induced NO generation in RAW 264.7 macrophages in a preliminary in vitro test. The aim of the present study was to evaluate the underlying mechanisms that mediate the inhibition of NO production by CYL-4d. This study would be useful for developing better compound structure through further modification of this molecule to improve anti-inflammatory activity. The results demonstrate that CYL-4d suppresses LPS-induced NO production and *iNOS* gene expression in macrophages mainly through the inhibition of mitogen-activated protein kinase (MAPK) kinase 4 (MEK4)/c-Jun NH_2-terminal kinase (JNK) pathway and the subsequent activator protein-1 (AP-1) transcriptional activity.

2. Materials and methods

2.1. Materials

Murine macrophage-like cell line RAW 264.7 was obtained from the American Type Culture Collection (Manassas, VA, USA). Murine microglial cell line BV-2 was kindly provided by Dr. J.-S. Hong (Neuropharmacology Section, NIEHS, Research Triangle Park, NC, USA). Dulbecco's modified Eagle medium (DMEM), penicillin-streptomycin, fetal bovine serum (FBS), SuperScript™ II reverse transcriptase system kit and LipofectAMINE transfection reagent were purchased from Invitrogen (Carlsbad, CA, USA). Anti-β-actin antibody and polyvinylidene difluoride membrane were obtained from Millipore (Billerica, MA, USA). ECL Western blotting reagent and poly(I)–poly(C) double-stranded RNA were purchased from GE Healthcare (Piscataway, NJ, USA). REzol™ C&T reagent was purchased from Protech Technology (Taiwan). SYBR Green PCR Master Mix reagent was obtained from Applied Biosystems (Foster City, CA, USA). DIG gel shift kit, CAT ELISA kit, β-Gal ELISA kit and nitrate reductase were purchased from Roche Applied Science (Mannheim, Germany). piNOS-CAT plasmid was obtained from Oxford Biomedical Research (Oxford, MI, USA). Antibodies against p65, IκBα, extracellular signal-regulated kinase (ERK) 2, p38 MAPK, phospho-JNK, JNK and proliferating cell nuclear antigen (PCNA) were purchased from Santa Cruz Biotechnology (Santa Cruz, CA, USA). Anti-iNOS antibody was obtained from BD Biosciences (Franklin Lakes, NJ, USA). Antibodies against phospho-ERK1/2, phospho-p38 MAPK, phospho-c-Jun, c-Jun, phospho-MEK3, MEK3, phospho-MEK4, and MEK4 were purchased from Cell Signaling Technology (Danvers, MA, USA). HRP-conjugated anti-mouse and anti-rabbit Ig were purchased from Pierce (Rockford, IL, USA). Oligonucleotide containing unmethylated CpG motifs was obtained from InvivoGen (Quebec, Canada). *N*-(3-aminomethyl)-benzylacetamidine (1400 W) was purchased from EMD Biosciences (San Diego, CA, USA). All other reagents and chemicals were obtained from Sigma–Aldrich (St. Louis, MO, USA).

2.2. Synthesis of CYL-4d

A mixture of 4-hydrazinoquinolone (1.75 g, 10 mmol) and cyclohex-2-enone (1.44 g, 15 mmol) in glacial acetic acid (50 ml) was stirred at room temperature for 36 h. The solvent was removed at reduced pressure, and ethylacetate was added to the residue. The precipitate that separated was collected by filtration, washed with H_2O, and dried to give CYL-4d (Fig. 1)

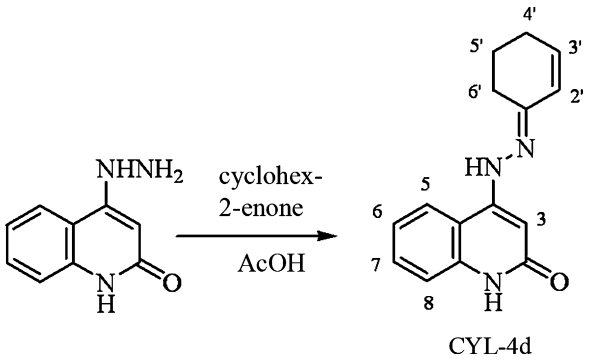

Fig. 1 – Synthesis of CYL-4d compound.

(2.19 g, 86%) as a pale yellow solid; m.p.: 254–255 °C. ^{1}H NMR (DMSO-d_6) δ 1.78 (quint, J = 6.6 Hz, 2H-C(5′)), 2.21 (m, 2H-C(4′)), 2.71 (t, J = 6.6 Hz, 2H-C(6′)), 6.13–6.30 (m, 3H-C(3, 2′ and 3′)), 7.13 (m, 1H-C(5)), 7.27 (m, 1H-C(4)), 7.48 (m, 1H-C(6)), 7.98 (m, 1H-C(8)), 9.15 (br s, 1-NH), 11.03 (br s, NH-C(4)); ^{13}C NMR (DMSO-d_6) δ 25.12, 27.76, 28.79, 93.85, 113.12, 116.49, 121.61, 122.95, 131.10, 135.22, 136.08, 139.71, 154.23, 161.69, 164.02. Anal. calcd. for $C_{15}H_{15}N_3O$: C, 71.13; H, 5.97; N, 16.59. Found: C, 71.24; H, 6.01; N, 16.60. CYL-4d (purity > 99%) was dissolved in dimethyl sulfoxide (DMSO).

2.3. Cell culture

RAW 264.7 cells and BV-2 cells were cultured in DMEM supplemented with 10% heat-inactivated FBS, 100 U/ml of penicillin and 100 μg/ml of streptomycin. Cells were grown at 37 °C under an atmosphere of 5% CO_2. Confluent cultures were passaged by trypsinization, and the passage number never exceeded 10. Rat alveolar macrophages were isolated by modidcation of the technique described previously [5]. Briefly, Sprague–Dawley rats (300–400 g) were anaesthetized with pentobarbital (50 mg/kg, i.p.). Lungs were lavaged via the tracheal cannula with 10 ml sterile cold phosphate buffer saline (PBS). The three lavage fractions were filtered though 70 μm mesh filter and then centrifuged (250 × g for 10 min at 4 °C). The cells pellet was resuspended in DMEM containing antibiotics without FBS and cultured onto 96-well plates at a density 2×10^5 cells/well. Cells were allowed to adhere for 60 min at 37 °C under 5% CO_2 and then gently washed with PBS to remove nonadherent cells. The purity of the alveolar macrophages was >95% as identified by Giemsa staining. Purified alveolar macrophages were cultured in DMEM supplemented with penicillin–streptomycin and 10% FBS. All experiments in the present study were performed under the guidelines of the Institutional Experimental Laboratory Animal Committee and were in strict accordance with the Guidelines for the Care and Use of Laboratory Animals as adopted and promulgated by the U.S. National Institute of Health.

2.4. Nitrite determination and iNOS activity assay

Cells (2×10^5, 1×10^5, and 2×10^5 cells/well for RAW 264.7 cells, BV-2 cells and rat alveolar macrophages, respectively) were seeded onto 96-well plates and allowed to adhere overnight. Cells were then treated with the test drug at 37 °C for 1 h before stimulation with 1 μg/ml of LPS for 24 h in a final volume of 0.2 ml. The production of NO was determined by measuring the accumulation of nitrite, the stable metabolite of NO, in culture medium based on the Griess reaction [6]. A standard nitrite curve was generated in the same fashion using $NaNO_2$. The iNOS activity in the cell lysate was measured as L-arginine- and NADPH-dependent generation of nitrite/nitrate [7]. Briefly, cells were stimulated with LPS for 16 h, and then harvested by lysis buffer (20 mM Tris–HCl, pH 7.5, 137 mM NaCl, 1 mM phenylmethylsulfonyl fluoride, 10 μg/ml each of aprotinin, leupeptin and pepstain A). The lysates (200 μg protein) were incubated in a 0.2 ml reaction mixture containing 20 mM Tris–HCl, pH 8.0, 2 mM NADPH, 2 mM L-arginine and 10 μM FAD in the presence or absence of test drugs for 3 h at room temperature. Nitrate formation in the reaction mixture was reduced to nitrite by incubation at 37 °C for 15 min with 0.1 U/ml of nitrate reductase, 0.1 mM NADPH and 5 μM FAD. The reaction was stopped by the addition of 10 U/ml of lactic dehydrogenase (LDH) and 10 mM pyruvate. Nitrite value of the control test (without NADPH/L-arginine) was subtracted from the experimental values.

2.5. Western blots

The proteins of cell lysate (40 μg) or nuclear extracts (10 μg) were separated by 7.5% (for iNOS, COX-2, β-actin) or 10% (for p65, PCNA, IκBα, phospho-c-Jun, c-Jun, phospho-ERK, ERK2, phospho-p38 MAPK, p38 MAPK, phospho-JNK, JNK, phospho-MEK3, MEK3, phospho-MEK4, MEK4) SDS-polyacrylamide gel electrophoresis and transferred to a polyvinylidene difluoride membranes. Membranes were blocked for 1 h at room temperature in TBST buffer (10 mM Tris–HCl, pH 8.0, 150 mM NaCl, and 0.1% Tween-20) containing 5% (w/v) nonfat milk, and then incubated overnight at 4 °C with a specific first antibody. After several washes, HRP-conjugated secondary antibody was added for a further 1 h incubation and blots were developed using an ECL detection kit. The signals were detected and quantified using a Luminescent Image Analyzer (Fujifilm LAS-3000) using MultiGauge software.

2.6. Quantitative real-time reverse transcription-polymerase chain reaction (Q-RT-PCR)

Total cellular RNA was extracted from RAW 264.7 cells using REzol™ C&T reagent and the cDNAs were synthesized from 2 μg of RNA of each sample using a SuperScript™ II reverse transcriptase system kit according to the manufacturer's protocol. Specific primers used were: iNOS (forward 5′-CAGC-TGGGCTGTACAAACCTT-3′ and reverse 5′-CATTGGAAGT-GAAGCGTTTCG-3′) and GAPDH (forward 5′-GGATGC-AGGGATGATGTTC-3′ and reverse 5′-TGCACCACCAACTGCT-TAG-3′). The Q-RT-PCR was carried in a 25 μl final volume containing: 125 ng cDNA sample, 2.5 μM primer pairs and 12.5 μl SYBR Green PCR Master Mix, and performed by an initial denaturation step at 95 °C for 10 min, followed by 40 cycles at 95 °C for 15 s and 60 °C for 60 s in an ABI PRISM HT7900 system sequence detector (Applied Biosystems). Each RNA sample was measured in duplication. The resulting iNOS mRNA abundance data were normalized against GAPDH mRNA abundance, and gene expression changes induced by the various treatments were determined by the $2^{-\Delta\Delta C_T}$ method [8]. In the mRNA degradation assay, cells were stimulated with LPS for 6 h. After being washed twice with PBS, the test drugs were added in the presence of 10 μg/ml of actinomycin D. Cells were then incubated further for 0, 2, 4, and 8 h. The RNA was extracted for Q-RT-PCR.

2.7. Transient transfection and reporter assay

CAT reporter gene expression under the control of the iNOS promoter (piNOS-CAT), NF-κB (p(NF-κB)$_3$-CAT), and AP-1 (p(AP-1)$_3$-CAT) was used for the in vitro transfection assays. A β-galactosidase reporter under the control of the SV40 early promoter and enhancer driving transcription of the bacterial

lacZ gene (pSV-β-galactosidase) was used as an internal control to normalize the reporter gene activity. RAW 264.7 cells were transfected by using LipofectAMINE reagent according to the instructions of the manufacturer. Twenty-four hours later, the culture medium was replaced, and cells were pretreated with a test drug for 1 h followed by stimulation with LPS. After 6 h (for NF-κB, AP-1 transcriptional activity) or 24 h (for iNOS promoter activity), the cells were lysed. The induction of CAT and β-galactosidase proteins in cell lysates was determined by using a CAT ELISA kit and a β-Gal ELISA kit, respectively, according to the instructions of the manufacturer.

2.8. Preparation of nuclear extracts and electrophoresis mobility shifted assay (EMSA)

Nuclear extracts were prepared as previously described [9]. Briefly, cells were washed twice with ice-cold PBS and resuspended in hypotonic buffer (10 mM HEPES, pH 7.9, 10 mM KCl, 0.1 mM EDTA, 0.1 mM EGTA, 1.5 mM $MgCl_2$, 1 mM dithiothreitol, 1 mM phenylmethylsulfonyl fluoride, 1 mM NaF and 1 mM Na_3VO_4). After the addition of 0.5% (v/v) Nonidet P-40 and vigorous vortexing for 10 s, the nuclei were pelleted by centrifugation (12,000 × *g* for 1 min at 4 °C). The collected nuclei pellet was resuspended in extraction buffer (20 mM HEPES, pH 7.9; 400 mM NaCl, 1 mM EGTA, 1 mM EDTA, 1 mM dithiothreitol, 1 mM NaF and 1 mM Na_3VO_4). After centrifugation (12,000 × *g* for 10 min at 4 °C), the supernatant was collected and stored at −70 °C. The oligonucleotide sequences 5′-CCAACTGGGGACTCTCCCTTTGGGAACA-3′ and 5′-GATCCGCTTGATGACTCAGCCGGAA-3′, corresponded to the consensus NF-κB and AP-1 sites, respectively, of the iNOS promoter [10,11] were synthesized. Nuclear extract (5 μg) was used for EMSA with a DIG gel shift kit according to the protocol of the manufacturer. The DNA/nuclear protein complex was separated from the DNA probe by electrophoresis on a native 6% polyacrylamide gel.

2.9. Statistical analysis

Data were analyzed by one-way analysis of variance (ANOVA) followed by the Bonferroni *t* test method for multi-group comparison tests. Analyses were considered significantly different at $P < 0.05$. Analysis of the regression line test was used to calculate IC_{50} values. Values are expressed as means ± S.D.

3. Results

3.1. Effects of CYL-4d on NO production and iNOS protein expression

Pretreatment of RAW 264.7 cells with CYL-4d concentration-dependently inhibited LPS-stimulated NO production (IC_{50} value about 16.9 μM) (Fig. 2A), whereas it alone (30 μM) did not

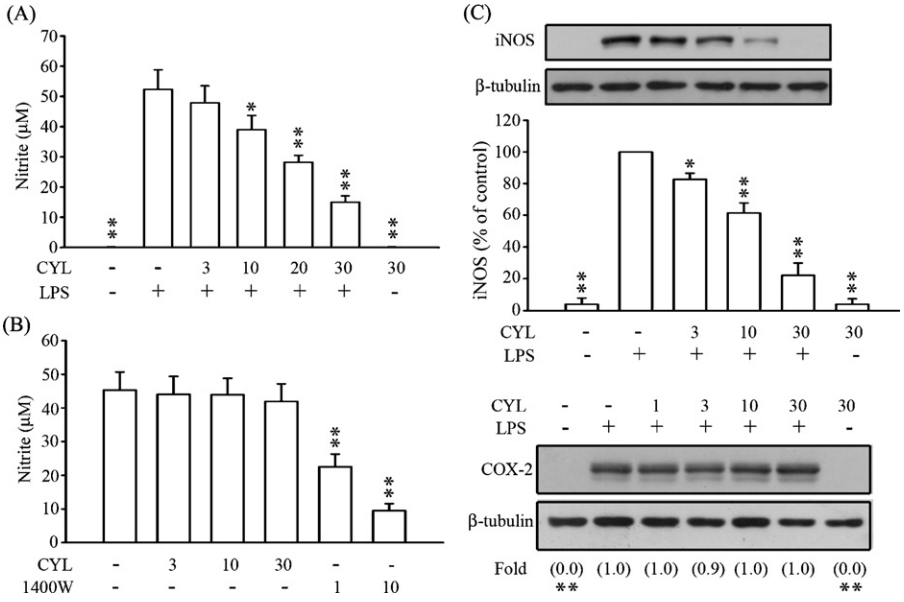

Fig. 2 – Effects of CYL-4d (CYL) on LPS-induced NO production, iNOS activity, iNOS and COX-2 protein expression in RAW 264.7 macrophages. (A) Cells were pretreated with the indicated concentrations (μM) of CYL for 1 h before stimulation for 24 h or no stimulation with LPS (1 μg/ml). The nitrite in the medium was determined. Values are expressed as means ± S.D. of four independent experiments. $^{*}P < 0.05$, $^{**}P < 0.01$, compared with the control value (2nd column). (B) Cell lysates were prepared after treatment of cells with LPS for 16 h, and then incubated with the indicated concentrations (μM) of CYL or 1400 W for iNOS activity assay. Values are expressed as means ± S.D. of four independent experiments. $^{**}P < 0.01$, compared with the control value (1st column). (C) Cells were pretreated with the indicated concentrations (μM) of CYL for 1 h before stimulation for 24 h or no stimulation with LPS. Whole-cell extracts were assayed for iNOS and COX-2 expression using Western blotting. The ratio of immunointensity between the iNOS, COX-2 and the loading control β-tubulin was calculated from four independent experiments. Values are expressed as means ± S.D. in iNOS experiment, and the fold increase in COX-2 expression is expressed. $^{*}P < 0.05$, $^{**}P < 0.01$, compared with the control value (2nd lane).

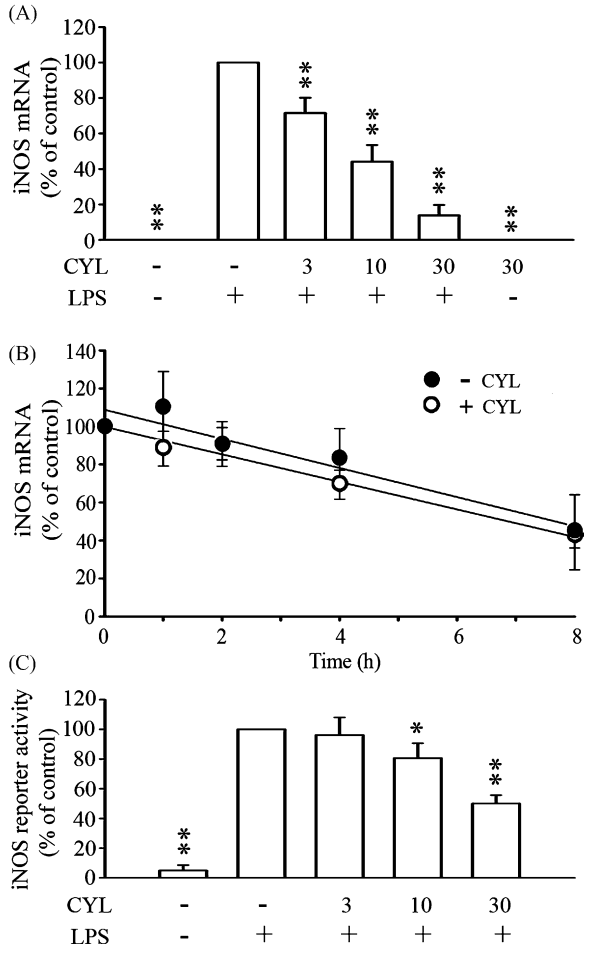

Fig. 3 – Effects of CYL-4d (CYL) on LPS-stimulated *iNOS* gene expression, RNA degradation and iNOS promoter activity in RAW 264.7 macrophages. (A) Cells were pretreated with the indicated concentrations (μM) of CYL for 1 h before stimulation for 6 h or no stimulation with LPS (1 μg/ml). The iNOS mRNA level was determined by Q-RT-PCR and normalized to the respective GAPDH mRNA level. Values are expressed as means ± S.D. of five independent experiments. $^{**}P < 0.01$, compared with the control value (2nd column). (B) Cells were stimulated with LPS 6 h before the addition of DMSO or 30 μM CYL in the presence of actinomycin D (10 μg/ml). At the indicated time after transcriptional blockade, iNOS mRNA level was analyzed by Q-RT-PCR. Values are expressed as means ± S.D. of four independent experiments. (C) The piNOS-CAT and pSV-β-galactosidase co-transfected cells were treated with the indicated concentrations (μM) of CYL for 1 h before stimulation for 24 h or no stimulation with LPS. The level of expressed CAT protein was quantified by an ELISA kit and normalized to the respective β-galactosidase activity. Values are expressed as means ± S.D. of four independent experiments. $^{*}P < 0.05$ or $^{**}P < 0.01$, compared with the control value (2nd column).

affect NO production ($P > 0.05$, compared with the LPS-untreated basal value). This inhibitory effect was not due to cell damage (viability > 95%) over reaction time as assessed in LDH release assay and in 3-(4,5-dimethylthiazol-2-yl)-2,5-diphenyltetrazolium bromide (MTT) reduction assay. Moreover, addition of CYL-4d (up to 30 μM) to the cell lysates of LPS-activated macrophages did not affect the expressed iNOS enzyme activity (Fig. 2B), whereas the selective iNOS inhibitor *N*-(3-aminomethyl)-benzylacetamidine (1400 W) showed a concentration-dependent inhibition.

In resting RAW 264.7 macrophages, iNOS and cyclooxygenase-2 (COX-2) proteins were undetectable. The pronounced expression of both iNOS and COX-2 proteins were demonstrated upon exposure to LPS for 24 h. CYL-4d attenuated iNOS protein expression, without affecting the COX-2 expression, in a concentration-dependent manner (IC_{50} value about 10.9 μM) (Fig. 2C). CYL-4d tested alone at the highest concentration (30 μM) had no effect on either iNOS or COX-2 proteins expression ($P > 0.05$, compared with the LPS-untreated basal value).

3.2. *Effect of CYL-4d on iNOS mRNA expression*

We next sought to determine whether *iNOS* gene expression was affected by CYL-4d in LPS-activated macrophages. The Q-RT-PCR analyses indicated that CYL-4d resulted in a concentration-dependent decrease in cellular iNOS mRNA levels (IC_{50} value about 7.3 μM) (Fig. 3A). CYL-4d (30 μM) alone did not affect iNOS mRNA expression ($P > 0.05$). After stimulation of cells with LPS for 6 h, the addition of CYL-4d in the presence of actinomycin D to inhibit transcription did not enhance iNOS mRNA degradation as judged by measuring half-life of the expressed iNOS mRNA ($T_{1/2}$ 6.7 ± 0.8 versus 7.6 ± 1.1 h for LPS-untreated basal value, $P > 0.05$) (Fig. 3B). In the transient co-transfection of RAW 264.7 cells with piNOS-CAT and pSV-β-galactosidase, expressions of CAT and galactosidase, respectively, were used to quantify the iNOS promoter activity. CYL-4d concentration-dependently reduced the LPS-induced iNOS promoter activity (IC_{50} value about 26.2 μM) (Fig. 3C).

3.3. *Effects of CYL-4d on the activation of NF-κB and AP-1*

To further elucidate the effect of CYL-4d on *iNOS* gene transcription, the activation of NF-κB and AP-1, two important transcription factors involved in murine *iNOS* gene expression [12], were examined. Analysis of reporter gene expression in RAW 264.7 cells, which were co-transfected with $p(NF\text{-}\kappa B)_3$-CAT or $p(AP\text{-}1)_3$-CAT and the internal control pSV-β-galactosidase, demonstrated that CYL-4d concentration-dependently inhibited AP-1 CAT expression (IC_{50} value about 20.8 μM), but had a lesser effect on NF-κB CAT expression (about 34% inhibition at 30 μM CYL-4d) (Fig. 4A).

We next undertook experiments to assess whether CYL-4d affects the transcription factors binding to DNA. LPS stimulation resulted in a significant increase in the DNA binding activity of both NF-κB and AP-1 as determined by EMSA (about 21.8% for LPS-untreated basal level versus 100% LPS-treated level for NF-κB, and 18.9% for LPS-untreated basal level versus 100% LPS-treated level for AP-1, both $P < 0.01$) (Fig. 4B). NF-κB exists in the cytosol of resting cells as homo- or heterodimer of the Rel family transcription factors [13]. The p65/50 and p50/50 complexes were identified using supershift analysis in our previous study on RAW 264.7 macrophages [14]. The specificity

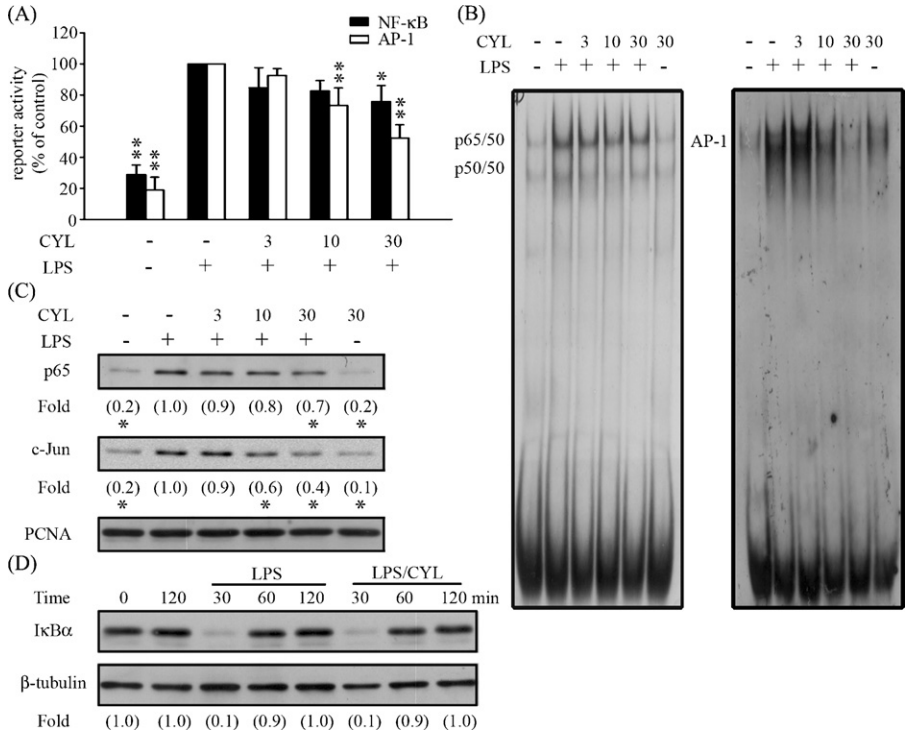

Fig. 4 – Effects of CYL-4d (CYL) on LPS-induced NF-κB and AP-1 activation and IκBα protein degradation in RAW 264.7 macrophages. (A) Cells were transiently co-transfected with pSV-β-galactosidase and p(NF-κB)$_3$-CAT or p(AP-1)$_3$-CAT reporter gene for 24 h, and then cells were pretreated with the indicated concentrations (μM) of CYL for 1 h before stimulation for 6 h or no stimulation with LPS (1 μg/ml). Cells were lysed to determine the expression of CAT and β-galactosidase. Values are expressed as means ± S.D. of four independent experiments. $^{*}P < 0.05$, $^{**}P < 0.01$, compared with the corresponding control values (2nd column group). (B) Cells were treated with the indicated concentrations of CYL for 1 h before stimulation for 1 h or no stimulation with LPS. The nuclear protein was extracted and tested for DNA binding of NF-κB or AP-1 by EMSA. The result shown is the representative of four independent experiments. (C) The p65, c-Jun and PCNA in nuclear extracts as mentioned above was determined by Western blot analysis and calculated in ratio, and the fold increase is expressed. $^{*}P < 0.01$, compared with the corresponding control values (lane 2). (D) Cells were treated with DMSO or 30 μM CYL for 1 h before stimulation or not stimulation with LPS for the indicated times. The protein levels of IκBα and β-tubulin was determined by Western blot analysis and calculated in ratio from four independent experiments, and the fold increase is expressed.

of binding was examined by competition with the unlabeled oligonucleotide (data not shown). CYL-4d attenuated the LPS-induced AP-1 binding in a concentration-dependent manner (IC_{50} value about 23.9 μM), but was less active in inhibiting the DNA binding of NF-κB (about 40% inhibition of the p65/50 complex binding at 30 μM CYL-4d, $P < 0.05$) (Fig. 4B). CYL-4d alone at the highest concentration tested (30 μM) failed to stimulate either AP-1 or NF-κB binding to DNA.

Translocation of the transcriptional factor into the nucleus is believed to be an essential event in activating genes with specific binding sites. Based on the immunoblot analysis, the nuclear levels of both NF-κB subunit p65 and AP-1 component c-Jun increased significantly 1 h after LPS stimulation. CYL-4d resulted in a concentration-dependent decrease in nuclear translocation of c-Jun (IC_{50} value about 11.4 μM) (Fig. 4C) but exhibited weak activity on that of p65 (about 39% inhibition at 30 μM CYL-4d). CYL-4d (30 μM) alone did not stimulate p65 and c-Jun nuclear translocation in RAW 264.7 cells. Upon cell activation, the phosphorylation and subsequent degradation of IκB leads to NF-κB activation. IκBα degradation was maximal after 30 min of exposure to LPS and then returned to basal levels within 1 h in RAW 264.7 macrophages. Pretreatment of cells with CYL-4d (30 μM) had no effect on the kinetics of IκBα degradation in response to LPS (Fig. 4D).

3.4. *Effects of CYL-4d on MAPK phosphorylation*

Stimulation of RAW 264.7 macrophages with LPS results in the activation of all three MAPKs, ERK, p38 MAPK and JNK [9]. The dual-phosphorylation of a conserved domain (TXY) of MAPKs by the upstream MEK1/2, MEK3/6 and MEK4/7 leads to activation of ERK, p38 MAPK and JNK, respectively [15]. The downstream targets of ERK and JNK include AP-1 [16]. Activation of JNK, in turn, phosphorylates the N-terminus (S63 and S73) of c-Jun protein leading to increases in activity [17]. The p38 MAPK is required for NF-κB-dependent gene expression [18]. Pretreatment of cells with CYL-4d at the concentrations tested (3–30 μM) had no inhibitory effect on the phosphorylation of either ERK or p38 MAPK, whereas it concentration-dependently attenuated the phosphorylation of JNK (IC_{50} value about 13.6 μM) in response to LPS stimulation (Fig. 5). In addition, CYL-4d inhibited the LPS-

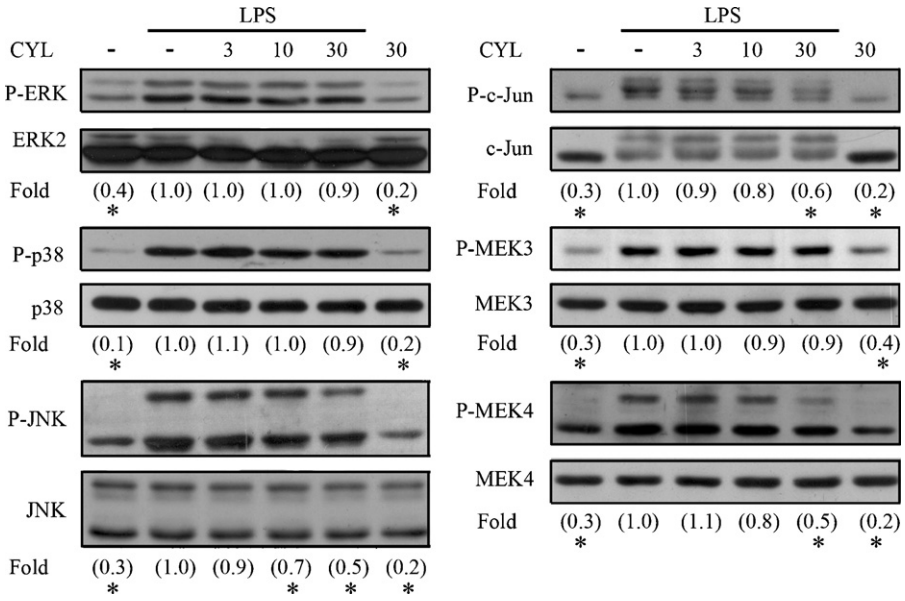

Fig. 5 – Effects of CYL-4d (CYL) on the activation of MEKs and MAPKs in RAW 264.7 macrophages. Cells were treated with the indicated concentrations (μM) of CYL for 1 h before stimulation for 20 min or no stimulation with LPS (1 μg/ml). MAPKs and MEKs were determined by specific antibodies, against the corresponding activated forms of MAPK or MEK. The blots above were then stripped and reprobed with the antibodies raised against the corresponding MAPKs or MEKs. The ratio of immunointensity between the phospho-MAPKs, phospho-MEKs and the corresponding loading controls was calculated from four independent experiments, and the fold increase is expressed. *$P < 0.01$, compared with the control value (lane 2).

induced phosphorylation of MEK4 (IC_{50} value about 24.9 μM) but not that of MEK3. The blockade of the MEK4/JNK transduction pathway by CYL-4d was confirmed as it also attenuated the LPS-induced c-Jun phosphorylation in the same concentration range (IC_{50} value about 22 μM) without affecting the MEK4, JNK and c-Jun proteins levels. CYL-4d (30 μM) alone did not affect the phosphorylation of MAPKs, MEK3/4 and c-Jun in RAW 264.7 cells.

3.5. *Effects of CYL-4d on various TLR ligands-induced iNOS expression*

Upon infection, pathogenic micro-organisms activate Toll-like receptors (TLRs), which are expressed on cells of the innate immune system, including macrophages. It is conceivable that LPS acting via TLR4 enhances the expression of inflammatory genes. We tested whether CYL-4d blocked iNOS expression in macrophages activated with TLRs ligands other than LPS. By exposing cells to peptidoglycans (a cell wall component of the Gram-positive bacteria for TLR2 stimulation), double-stranded RNA (a synthetic poly(I)–poly(C) for TLR3 stimulation) or a synthetic oligonucleotide containing unmethylated CpG motifs (for TLR9 stimulation), all three TLRs ligands induced iNOS protein expression in RAW 264.7 cells. CYL-4d resulted in a concentration-dependent decrease in iNOS expression in response to ligands with similar IC_{50} values (about 8.2, 8.5 and 6.3 μM for peptidoglycans, double-stranded RNA and oligonucleotides containing unmethylated CpG motifs, respectively) (Fig. 6). Under the same culture conditions, CYL-4d (30 μM) alone showed no activity in iNOS expression.

3.6. *Effects of CYL-4d on NO production from BV-2 microglial cells and alveolar macrophages*

We next addressed the question of whether the inhibitory effect of CYL-4d on NO production is restricted to RAW 264.7 cells, so the culture cells were replaced by BV-2 murine microglial cells and primary rat alveolar macrophages. Stimulation with LPS effectively increased the NO production as judged from the accumulation of nitrite in the culture medium of BV-2 microglia and alveolar macrophages, and these responses were suppressed by CYL-4d in the same concentration range with even greater inhibitory potencies (IC_{50} values about 3.3 and 2.6 μM, respectively) compared to the inhibition of NO production in RAW 264.7 cells (Fig. 7). This inhibitory effect was not due to cell damage (viability >95%) as assessed in MTT reduction assay.

4. Discussion

Macrophages play particularly important roles in inflammation via the production of many pro-inflammatory molecules, including NO. The overproduction of NO can be harmful and results in various inflammatory diseases. Therefore, pharmacological interference with NO production is postulated to be useful to alleviate numerous disease states that are mediated by excessive and/or protracted activation of macrophages. In the present study, we demonstrated that a novel synthetic compound CYL-4d inhibits LPS-induced NO production in RAW 264.7 cells, a widely used macrophage-like cell line. This inhibitory effect is not mediated by the cytotoxic effect on

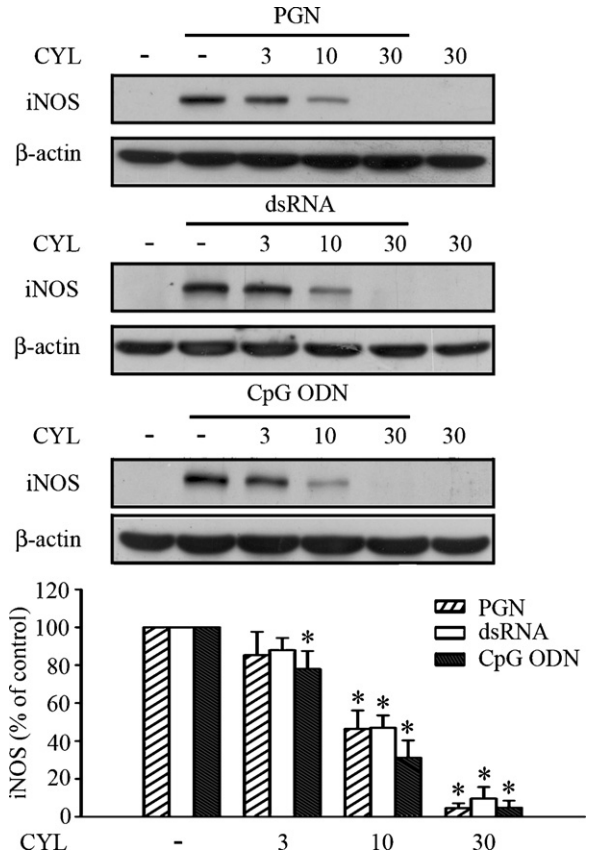

Fig. 6 – Effects of CYL-4d (CYL) on TLR ligands-induced iNOS protein levels in RAW 264.7 macrophages. Cells were treated with the indicated concentrations (μM) of CYL for 1 h before stimulation for 24 h or no stimulation with peptidoglycans (PGN, 10 μg/ml), double-stranded RNA (dsRNA, 50 μg/ml) or oligonucleotides containing unmethylated CpG motifs (CpG ODN, 10 μg/ml). The whole-cell lysates were analyzed by Western blot analysis using antibody against iNOS protein. The ratio of immunointensity between the iNOS and the loading control β-actin was calculated. Values are expressed as means ± S.D. of four independent experiments. *P < 0.05, compared with the corresponding control values (1st column group).

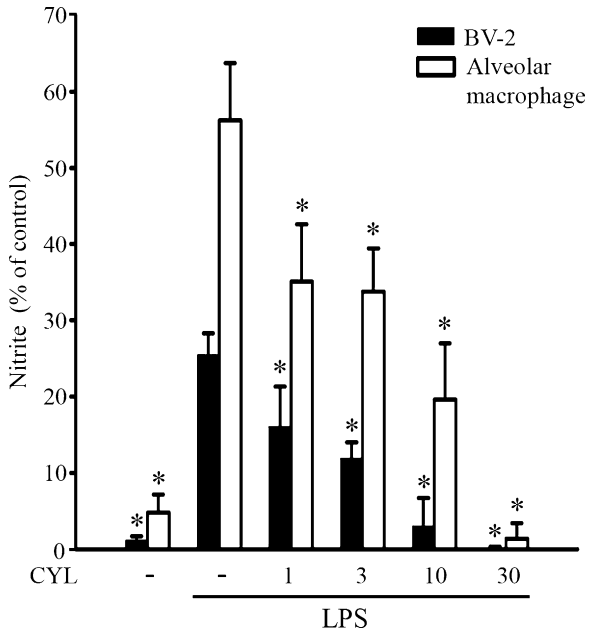

Fig. 7 – Effects of CYL-4d (CYL) on LPS-stimulated NO production in BV-2 microglia and rat alveolar macrophages. Cells were pretreated with the indicated concentrations (μM) of CYL for 1 h before stimulation for 24 h or no stimulation with LPS (1 μg/ml). The nitrite in the medium was determined. Values are means ± S.D. of four independent experiments. *P < 0.01, compared with the corresponding control values (2nd column group).

macrophages. The result that CYL-4d had no appreciable inhibitory effect on the expressed iNOS enzyme activity suggests the upstream inhibition. The parallel inhibition of iNOS protein and mRNA expression, without affecting the stability of the expressed iNOS mRNA, in LPS-stimulated cells implies that the blockade of transcription step could have a critical role. In line with this notion, CYL-4d at a similar concentration range blocked LPS-induced iNOS promoter activity in piNOS-CAT-transfected cells.

There are a number of binding sites for transcription factors located in the promoter of the *iNOS* gene, in which NF-κB and AP-1 are principally involved for LPS-mediated NO production [12]. Inactive NF-κB constitutively binds to inhibitory IκB proteins in the cytoplasm. When LPS acting via Toll-like receptor (TLR) 4, the receptors dimerize and undergo conformational changes required for the recruitment and activation of downstream signaling molecule cascade. After activation of IκB kinase (IKK), the subsequent NF-κB activation results from phosphorylation, ubiquitination, and proteasome-mediated degradation of IκB proteins, followed by translocation of NF-κB into the nucleus to activate genes with NF-κB binding sites [19].

CYL-4d was found to exhibit weak inhibitory effect on LPS-induced NF-κB transcriptional activity in $p(NF\text{-}\kappa B)_3$-CAT-transfected cells. This, together with the slight inhibition by CYL-4d of the NF-κB DNA binding and p65 nuclear translocation (about 30–40% inhibition for all three responses at 30 μM CYL-4d, $P < 0.05$) as assessed in the nuclear extract of LPS-activated RAW 264.7 cells with the EMSA assay and Western blot analysis, respectively, indicates that the modest but significant inhibition of NF-κB activation is not the key target during CYL-4d inhibition of NO production. Interestingly, CYL-4d failed to elicit detectable changes in the time course of LPS-induced IκBα degradation. This finding contradicts the target site for IKK in CYL-4d inhibition of NF-κB activation. It is conceivable that the IκB-free NF-κB is recognized by karyopherin α and subsequently interacts with karyopherin β and the small GTP binding protein, Ran in the cytoplasm [20,21]. These complexes bind to the nuclear pore and are then transported into the nucleus. It is plausible that the inhibition of NF-κB transcriptional activity by CYL-4d can be attributed to the blockade of NF-κB nuclear import, but this remains to be investigated. Previous studies have also demonstrated that

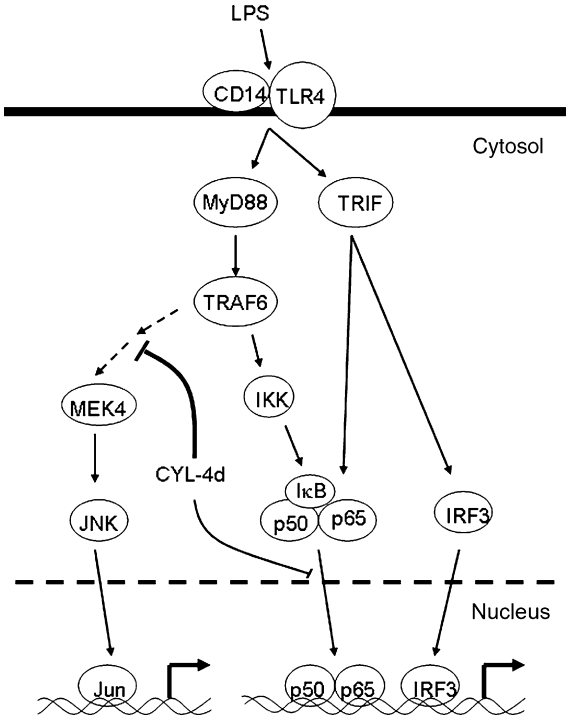

Fig. 8 – Schematic diagram showing the mechanisms underlying the inhibition by CYL-4d. Arrows indicate the TLR4 signalling. The signalling molecules generally employed in mediating activation of the transcription factors NF-κB and AP-1 and the MAPKs are indicated. The relationships yet to be clearly demonstrated in macrophages are indicated as broken arrows. Some additional signalling molecules in these pathways have been omitted for the sake of clarity. Blunt lines indicate the inhibition by CYL-4d (The thick line indicates the major inhibitory response, while thinner line indicates the lesser response). IRF3, interferon-regulatory factor 3; TRAF6, tumour-necrosis-factor-receptor-associated factor 6; TRIF, TIR-domain-containing adaptor protein inducing IFN-β.

the synthetic peptide SN50 and a novel compound JSH-23 interfered LPS-induced nuclear translocation of NF-κB without affecting IκB degradation [22,23].

AP-1 is composed of members of the Jun (c-Jun, JunB, and JunD) and Fos (c-Fos, FosB, Fra-1, and Fra-2) families [24]. The most common are the c-Jun/c-Fos heterodimers that bind to the TPA-response elements (AP-1 sites) in the promoters of various genes [25]. However, the use of supershift assays to identify the components of AP-1 indicated that c-Jun but not c-Fos is part of this complex at the AP-1 site in RAW 264.7 cells [26]. The results that CYL-4d markedly reduced the LPS-induced AP-1 DNA binding and c-Jun nuclear translocation in RAW 264.7 cells together with the substantial inhibition of AP-1 transcriptional activity in $p(AP\text{-}1)_3$-CAT-transfected cells provide clear evidence of inhibition of AP-1 activation by CYL-4d. Moreover, the inhibition of AP-1 activation and NO production in the same concentration range of CYL-4d strongly supports the critical role of AP-1.

Three major subfamilies of MAPK cascades, i.e., ras-raf1-MEK1/2-ERK1/2, rac-MEKK1-MEK4/7-JNK1/2 and MEK3/6-p38 MAPK, have been defined [15]. MAPKs transmit signals in the form of sequential phosphorylation events. LPS induces all three MAPK pathways activation in RAW 264.7 macrophages [9] and these pathways can regulate gene expression in LPS-activated macrophages [27]. However, the mechanisms by which MAPKs are activated by TLRs are incompletely understood. Pharmacological approaches with MAPK-specific inhibitors have demonstrated that the JNK, but not p38 and ERK, pathway is required for LPS-induced NO production and iNOS expression in RAW 264.7 macrophages [28,29]. CYL-4d did not affect the phosphorylation of ERK and p38 MAPK. In contrast, CYL-4d effectively decreased the phosphorylation of JNK and its downstream target c-Jun at the concentration range closely matched the concentration dependence of inhibition of AP-1. The parallel inhibition of the phosphorylation of JNK and MEK4 implies that CYL-4d targeted the upstream activator. Thus, the inhibition of AP-1 activation by CYL-4d appears attributable to the blockade of MEK4-JNK pathway. The result that CYL-4d did not affect p38 MAPK phosphorylation is supported by the lack of effect on the phosphorylation of MEK3 in response to LPS. It has been proposed that JunB, a negative transcriptional regulator, competes with c-Jun for JNK and DNA binding [30], leading to a reduction in c-Jun activation. Based on current data, the possibility of a role for JunB in CYL-4d inhibition of AP-1 cannot be excluded.

In addition to NO, macrophages also release prostaglandins, which are COX products. At least two genetically distinct COX isoforms: the constitutive COX-1 and the inducible COX-2 have been identified [31]. Recent studies have demonstrated that CCAAT-enhancer binding protein β (C/EBPβ) and cyclic-AMP response element binding protein (CREB) play a major role during the initial stage of COX-2 transcriptional activation [32,33] and LPS activates C/EBPβ and CREB via p38 MAPK and ERK. Moreover, aspirin and sodium salicylate selectively inhibit C/EBPβ activation, thereby suppressing the expression of COX-2 induced by LPS, but not TNFα, which depends largely on NF-κB activation [34]. The lack of inhibitory effect on the phosphorylation of ERK and p38 MAPK could account for why CYL-4d was unable to attenuate LPS-induced COX-2 expression. Stimulation of TLR4 by LPS activates the IKK complex which triggers the phosphorylation and the subsequent degradation of p105 to liberate tumor progression locus-2 (TPL-2), which in turn phosphorylates and activates MEK-ERK pathway [35]. The failure of CYL-4d to inhibit ERK phosphorylation implies intact IKK activity. This data also supports the above notion that CYL-4d did not affect the NF-κB activation, but probably interfered with its nuclear translocation.

To evaluate whether the inhibitory action of CYL-4d is restricted to LPS-TLR4 signaling, experiments with various TLRs activators other than LPS were performed. It is conceivable that activation of TLR4 elicits two distinct downstream intracellular signaling pathways, myeloid differentiation primary-response protein 88 (MyD88)-dependent and -independent, whereas the TLR2 and TLR9 ligands through the MyD88-dependent pathway, activate transcription factors [19]. Although MyD88 has been reported to be involved in TLR3 signaling, TLR3 seems to transduce its signals mainly through the MyD88-independent pathway. CYL-4d inhibited the iNOS protein expression caused by three TLRs ligands, including peptidoglycans (for TLR2), double-stranded RNA (for

TLR3) and a synthetic oligonucleotide containing unmethylated CpG motifs (for TLR9), with IC_{50} values similar to the concentration required for the inhibitory effect on LPS-induced response, indicating that the suppressive effects of CYL-4d are not restricted to LPS stimulation and have nothing to do with MyD88.

Microglial cells, the resident brain macrophages, are involved in immune surveillance and host defense against infectious agents [36]. Pathological microglial activation, in response to LPS, is believed to contribute to progressive damage in neurodegenerative diseases through the release of pro-inflammatory factors, including NO [37]. Alveolar macrophages are the first line of defense against respiratory pathogens [38]. The results that CYL-4d inhibited the NO production in both murine BV-2 microglial cell line and the rat primary alveolar macrophages in response to LPS reveal that suppressive effects of CYL-4d are not restricted to RAW 264.7 cells or immortal macrophage-like cells; it can occur in primary macrophages. Thus, it is expected that CYL-4d will have similar effects in vivo. The low IC_{50} values obtained from both BV-2 microglia and alveolar macrophages experiments make CYL-4d to a potential candidate molecule for developing anti-inflammatory drugs to alleviating neurodegeneration and lung injury. In fact, CYL-4d also exhibited the parallel inhibition of LPS-induced iNOS protein expression and iNOS mRNA abundance in BV-2 microglia (data not shown) with similar IC_{50} values to NO production. It is plausible that CYL-4d inhibition of NO production in BV-2 microglia as well as in RAW 264.7 macrophages might act via a similar intracellular signal mechanism.

In summary, we have demonstrated that inhibition of LPS-induced NO production by CYL-4d in RAW 264.7 macrophages is attributed mainly to the down-regulation of AP-1 activity through the blockade of the upstream activator of MEK4-JNK-c-Jun signaling pathway, and partly to the suppression of NF-κB activity probably through the blockade of nuclear translocation (Fig. 8). Further investigation is required to find out the molecular target(s) of CYL-4d in the AP-1 pathway and to find out whether this compound can suppress other inflammatory reactions mediated by macrophages in vitro and in vivo.

Acknowledgements

This work was supported in part by grants from the National Science Council (NSC-94-2320-B-075A-005) and Taichung Veterans General Hospital (TCVGH-927322D, TCVGH-957311C), Taiwan, ROC.

REFERENCES

[1] Marletta MA. Nitric oxide synthase structure and mechanism. J Biol Chem 1993;268:12231–4.
[2] Xie Q, Nathan C. The high-output nitric oxide pathway: role and regulation. J Leukoc Biol 1994;56:576–82.
[3] McCartney-Francis N, Allen JB, Mizel DE, Albina JE, Xie QW, Nathan CF, et al. Suppression of arthritis by an inhibitor of nitric oxide synthase. J Exp Med 1993;178:749–54.
[4] Chen YL, Chung CH, Chen IL, Chen PH, Jeng HY. Synthesis and cytotoxic activity evaluation of indolo-, pyrrolo-, and benzofuro-quinolin-2(1*H*)-ones and 6-anilinoindoloquinoline derivatives. Bioorg Med Chem 2002;10:2705–12.
[5] Liu SH, Tzeng HP, Kuo ML, Lin-Shiau SY. Inhibition of inducible nitric oxide synthase by β-lapachone in rat alveolar macrophages and aorta. Br J Pharmacol 1999;126:746–50.
[6] Minghetti L, Nicolini A, Polazzi E, Creminon C, Maclouf J, Levi G. Inducible nitric oxide synthase expression in activated rat microglial cultures is downregulated by exogenous prostaglandin E_2 and by cyclooxygenase inhibitors. Glia 1997;19:152–60.
[7] Wang MJ, Huang HM, Chen HL, Kuo JS, Jeng KC. Dehydroepiandrosterone inhibits lipopolysaccharide-induced nitric oxide production in BV-2 microglia. J Neurochem 2001;77:830–8.
[8] Livak KJ, Schmittgen TD. Analysis of relative gene expression data using real-time quantitative PCR and the $2^{-\Delta\Delta C}$T method. Methods 2001;25:402–8.
[9] Tsao LT, Tsai PS, Lin RH, Huang LJ, Kuo SC, Wang JP. Inhibition of lipopolysaccharide-induced expression of inducible nitric oxide synthase by phenolic (3*E*)-4-(2-hydroxyphenyl)but-3-en-2-one in RAW 264.7 macrophages. Biochem Pharmacol 2005;70:618–26.
[10] Velasco M, Diaz-Guerra MJ, Diaz-Achirica P, Andreu D, Rivas L, Bosca L. Macrophage triggering with cecropin A and melittin-derived peptides induces type II nitric oxide synthase expression. J Immunol 1997;158:4437–43.
[11] Tsi CJ, Chao Y, Chen CW, Lin WW. Aurintricarboxylic acid protects against cell death caused by lipopolysaccharide in macrophages by decreasing inducible nitric-oxide synthase induction via IκB kinase, extracellular signal-regulated kinase, and p38 mitogen-activated protein kinase inhibition. Mol Pharmacol 2002;62:90–101.
[12] Hatziieremia S, Gray AI, Ferro VA, Paul A, Plevin R. The effects of cardamonin on lipopolysaccharide-induced inflammatory protein production and MAP kinase and NF-κB signalling pathways in monocytes/macrophages. Br J Pharmacol 2006;149:188–98.
[13] Ghosh S, May MJ, Kopp EB. NF-κB and Rel proteins: evolutionarily conserved mediators of immune responses. Annu Rev Immunol 1998;16:225–60.
[14] Tsao LT, Lee CY, Huang LJ, Kuo SC, Wang JP. Inhibition of lipopolysaccharide-stimulated nitric oxide production in RAW 264.7 macrophages by a synthetic carbazole, LCY-2-CHO. Biochem Pharmacol 2002;63:1961–8.
[15] Krens SFG, Spaink HP, Snaar-Jagalska BE. Functions of the MAPK family in vertebrate-development. FEBS Lett 2006;580:4984–90.
[16] Cano E, Mahadevan LC. Parallel signal processing among mammalian MAPKs. Trends Biochem Sci 1995;20:117–22.
[17] Derijard B, Hibi M, Wu IH, Barrett T, Su B, Deng T, et al. JNK1: a protein kinase stimulated by UV light and Ha-Ras that binds and phosphorylates the c-Jun activation domain. Cell 1994;76:1025–37.
[18] Carter AB, Knudtson KL, Monick MM, Hunninghake GW. The p38 mitogen-activated protein kinase is required for NF-κB-dependent gene expression. The role of TATA-binding protein (TBP). J Biol Chem 1999;274:30858–63.
[19] Akira S, Takeda K. Toll-like receptor signalling. Nat Rev Immunol 2004;4:499–511.
[20] Torgerson TR, Colosia AD, Donahue JP, Lin YZ, Hawiger J. Regulation of NF-κB, AP-1, NFAT, and STAT1 nuclear import in T lymphocytes by noninvasive delivery of peptide carrying the nuclear localization sequence of NF-κB p50. J Immunol 1998;161:6084–92.

[21] Moroianu J. Distinct nuclear import and export pathways mediated by members of the karyopherin β family. J Cell Biochem 1998;70:231–9.
[22] Kolenko V, Bloom T, Rayman P, Bukowski R, His E, Finke J. Inhibition of NF-κB activity in human T lymphocytes induces caspase-dependent apoptosis without detectable activation of caspase-1 and -3. J Immunol 1999;163:590–8.
[23] Shin HM, Kim MH, Kim BH, Jung SH, Kim YS, Park HJ, et al. Inhibitory action of novel aromatic diamine compound on lipopolysaccharide-induced nuclear translocation of NF-κB without affecting IκB degradation. FEBS Lett 2004;571:50–4.
[24] Hambleton J, Weinstein SL, Lem L, DeFranco AL. Activation of c-Jun N-terminal kinase in bacterial lipopolysaccharide-stimulated macrophages. Proc Natl Acad Sci USA 1996;93:2774–8.
[25] Karin M, Liu ZG, Zandi E. AP-1 function and regulation. Curr Opin Cell Biol 1997;9:240–6.
[26] Martin CB, Martin BK. Characterization of the murine C3a receptor enhancer-promoter: expression control by an activator protein 1 sequence and an Ets-like site. J Immunol 2005;175:3123–32.
[27] Guha M, Mackman N. LPS induction of gene expression in human monocytes. Cell Signal 2001;13:85–94.
[28] Paul A, Cuenda A, Bryant CE, Murray J, Chilvers ER, Cohen P, et al. Involvement of mitogen-activated protein kinase homologues in the regulation of lipopolysaccharide-mediated induction of cyclo-oxygenase-2 but not nitric oxide synthase in RAW 264.7 macrophages. Cell Signal 1999;11:491–7.
[29] Uto T, Fujii M, Hou DX. 6-(Methylsulfinyl)hexyl isothiocyanate suppresses inducible nitric oxide synthase expression through the inhibition of Janus kinase 2-mediated JNK pathway in lipopolysaccharide-activated murine macrophages. Biochem Pharmacol 2005;70:1211–21.
[30] Deng T, Karin M. JunB differs from c-Jun in its DNA-binding and dimerization domains, and represses c-Jun by formation of inactive heterodimers. Genes Dev 1993;7:479–90.
[31] Lee SH, Soyoola E, Chanmugam P, Hart S, Sun W, Zhong H, et al. Selective expression of mitogen-inducible cyclooxygenase in macrophages stimulated with lipopolysaccharide. J Biol Chem 1992;267:25934–8.
[32] Eliopoulos AG, Dumitru CD, Wang CC, Cho J, Tsichlis PN. Induction of COX-2 by LPS in macrophages is regulated by Tpl2-dependent CREB activation signals. EMBO J 2002;21:4831–40.
[33] Wu KK. Transcription-based COX-2 inhibition: a therapeutic strategy. Thromb Haemost 2006;96:417–22.
[34] Wu KK, Liou JY, Cieslik K. Transcriptional control of COX-2 via C/EBPβ. Arterioscler Thromb Vasc Biol 2005;25:679–85.
[35] Beinke S, Ley SC. Functions of NF-κB1 and NF-κB2 in immune cell biology. Biochem J 2004;382:393–409.
[36] Gonzalez-Scarano F, Baltuch G. Microglia as mediators of inflammatory and degenerative diseases. Annu Rev Neurosci 1999;22:219–40.
[37] Liu B, Hong JS. Role of microglia in inflammation-mediated neurodegenerative diseases: mechanisms and strategies for therapeutic intervention. J Pharmacol Exp Ther 2003;304:1–7.
[38] Sibille Y, Reynolds HY. Macrophages and polymorphonuclear neutrophils in lung defense and injury. Am Rev Respir Dis 1990;141:471–501.